SLIM-Based High-Resolution Ion Mobility Reveals New Structural Insights into Isomeric Vitamin D Metabolites and their Isotopologues

*Selena Kingsley,[1,2] Makenna Hoover,[1] Terra Pettit-Bacovin,[1] Anna Rose Sawyer,[1] Christopher D. Chouinard[1]**

[1]Clemson University, Department of Chemistry; Clemson, SC, USA 29634

[2]Lake Superior State University, Department of Chemistry; Sault Sainte Marie, MI, USA 49783

Corresponding author email: cchouin@clemson.edu

KEYWORDS: Vitamin D; Ion Mobility-Mass Spectrometry; Structures for Lossless Ion Manipulations (SLIM)

ABSTRACT

Testing for vitamin D deficiency remains a high-volume clinical assay, much of which is done using mass spectrometry-based methods to alleviate challenges in selectivity associated with immunoassays. Ion mobility-mass spectrometry (IM-MS) has been proposed as a rapid alternative to traditional LC-MS/MS methods, but understanding the structural ensemble that contributes to the ion mobility behavior of this molecular class is critical. Herein we demonstrate the first application of high-resolution Structures for Lossless Ion Manipulations (SLIM) IM separations of several groups of isomeric vitamin D metabolites. Despite previous IM studies of these molecules, the high resolving power of SLIM (R_p ~ 200) has revealed additional conformations for several of the compounds. The highly similar collision cross sections (CCS), some differing by as little as 0.7%, precluded adequate characterization with low-resolution IM techniques where, in some cases, wider than expected peak widths and/or subtle shoulders may have hinted at their presence. Importantly, these newly resolved peaks often provided a unique mobility that could be used to separate isomers and provides potential for their use in quantification. Lastly, the contribution of isotopic labeling to arrival time distribution for commonly used ^{13}C- and deuterium-labeled internal standards was explored. Minor shifts of ~0.2-0.3% were observed, and in some instances these shifts were specific to the conformer being measured (i.e., ‘closed’ vs. ‘open’). Accounting for these shifts is important during raw data extraction to ensure reproducible peak area integration, which will be a critical consideration in future quantitative applications.

INTRODUCTION

Vitamin D and its metabolites are secosteroid hormones that collectively regulate the absorption of calcium and phosphate in the body.[1] Subclasses of D2 and D3 metabolites differ in their biological origin (plant-derived vs. animal-derived, respectively), but serve the same functions in human metabolic processes such as regulating the immune, endocrine, cardiovascular, and nervous systems, as well as cognitive health.[2] As such, these metabolites are often reported clinically as combined total concentrations of 25-hydroxyvitamin D2 (25OHD2) and 25OHD3. Deficiency or insufficiency are defined as total 25OHD concentration less than 20 ng/ml (50 nmol/liter) or between 21–29 ng/ml (525–725 nmol/liter),[3] respectively, and are well known to cause health complications including osteomalacia, increased bone fractures, or osteoporosis; these risks are especially present in young children and the elderly. The most common clinical methods used to quantify vitamin D status are immunoassays and chromatographic/mass spectrometric methods.[4] While fast and inexpensive, immunoassays lack selectivity and are prone to interferences that can result in variability in quantification.[5,6] Such interferences include endogenous isomers, such as the C3 epimers of 25OHD3/25OHD2, which have been shown to contribute less to calcium homeostasis and have been implicated in certain disease states.[7] Additional clinical targets also suffer from isomeric interferences, such as 1,25-dihydroxyvitamin D (the active form of vitamin D) and 24,25-dihydroxyvitamin D. Both tandem mass spectrometry and chromatographic methods are similarly challenged to resolve these species, especially on the clinical timescale (generally ≤2 mins).[8,9] Numerous references detail analytical considerations for LC-MS/MS-based quantification of vitamin D metabolites and how these interferences can lead to systematic bias, including a recent tutorial by Volmer et al.[10,11]

One method proposed to overcome the issues associated with isomeric/isobaric interferences is ion mobility-mass spectrometry (IM-MS), which has recently shown promise in clinical applications including for the analysis of vitamin D.[12,13] IM rapidly separates gas-phase

ions based on differences in their size, shape, and charge when exposed to an electrical field. As such, IM provides the ability to resolve isomers, and to do so on a relatively rapid timescale which ranges between tens-hundreds of milliseconds, in comparison with the several minutes required for chromatography.[14] Qi et al. demonstrated the first analysis of 25-hydroxyvitamin D by IM, specifically differential ion mobility spectrometry (DMS), as a means to filter isobaric interferences (e.g., pentaerythritol) when using low-resolution mass spectrometers (i.e., triple quadrupole-based analyzers).[10] Not long after, a jointly filed patent by Roche Diagnostics Operations, Inc. and Owlstone Medical Limited broadly described the use of high field asymmetric waveform IMS (FAIMS) for the separation of 25OHD3 and its epimer as sodiated ions;[15] similar studies by Chouinard et al. using low field drift tube IMS (DTIMS) confirmed the presence of multiple gas-phase conformations of sodiated 25OHD3 and 25OHD2 ('open' and 'closed'), as aided by computational modeling, which allowed for differentiation from their respective epimers.[16] The ratio of these conformers was later shown to be dependent on experimental variables such as the metal cation used and ion source conditions.[17,18] An important collaborative study by Oranzi et al. further investigated this conformational ratio with several commercial instruments including atmospheric- and low-pressure DTIMS, traveling wave IMS (TWIMS), trapped IMS (TIMS), and high field asymmetric waveform IMS (FAIMS);[19] these results demonstrated the variability in separation and identification of conformers, highlighting the importance of adequately sharing experimental parameters for collection of IM data with different platforms. Oranzi et al. then proceeded to develop a rapid, targeted LC-IM-HRMS method for quantification of 25OHD3 and 25OHD2 by filtering out their interfering epimers, which yielded quantitative information over a clinically relevant range from 2-500 ng/mL.[20] More recent method development studies have focused on DMS-based approaches to improve specificity and sensitivity for a range of vitamin D metabolites.[21,22]

Despite these various works, comprehensive analysis of these compounds has yet to be undertaken using Structures for Lossless Ion Manipulations (SLIM). This recently developed IM technique allows for measurement of mobility as ions are propelled by a traveling wave through serpentine paths patterned on printed circuit boards.[23–27] The serpentine nature allows for long-path separations (≥13 m) that provide resolving power of R_p >200. Numerous small molecule applications have been demonstrated including separation of isomeric glycans,[28] amino acids and peptides,[29,30] bile acids,[31] lipids,[32,33] and most recently synthetic cannabinoid metabolites.[34] An important consideration for the proposed coupling of high-resolution IM with quantitative clinical analysis is the anticipated arrival time shift for isotopically-labeled internal standards relative to their unlabeled equivalents (i.e., isotopologues), based on differences in their reduced mass.[35–37] Such separations have been observed previously with SLIM for tetraalkylammonium ions, amino acids, and peptide isotopologues,[35,38] as well as with other low-field[39–42] and high-field IM platforms.[43–47] Williamson et al.[41] used a cyclic IMS (cIMS) device to measure structurally-specific mass distribution-based isotopic shifts for 25-hydroxyvitamin D3, among other compounds, and interestingly they determined that the previously identified 'closed' and 'open' conformations[16] had different relative shifts, with the 'closed' showing only a 0.17% relative increase in arrival time in comparison with the 0.28% shift for the 'open' conformer.[41] Because there is no difference in reduced mass between the conformers, they attributed the arrival time shift to the change in center of mass owing to the position of the $^{13}C_5$ labeling on the end of the molecule; this positioning would be further from the center of mass in the 'open' conformer. A more recent paper from Williamson et al. attempted to isolate the contribution of moment of inertia (which itself is calculated in relation to center of mass) by investigating mobility shifts of differentially labeled tetrapropylammonium isotopologues (all with the same center of mass, but different moments of inertia).[48] They concluded that isolated changes in moment of inertia could indeed contribute to proportional shifts in arrival time, and therefore collision cross section (CCS). In the present study, we show the first comprehensive analysis of a wide range of vitamin D metabolites using SLIM

IM-MS, and also further investigate the isotopic shifts associated with labeled isotopologue compounds.

EXPERIMENTAL SECTION

Chemicals and Reagents

Standards of Vitamin D metabolites and their isotopologues were provided by Advanced Stable Isotope (ASI) Chemicals (Cheyney, PA) and included: 25-hydroxyvitamin D2 (100 ug/mL), [$^{13}C_5$]-25-hydroxyvitamin D2 (50 ug/mL), [$^{13}C_5$]-3-epi-25 hydroxyvitamin D2 (10 ug/mL), 25-hydroxyvitamin D3 (100 ug/mL), [$^{13}C_5$]-25-hydroxyvitamin D3 (50 ug/mL), 3-epi-25-hydroxyvitamin D3 (50 ug/mL), and [$^{13}C_5$]-3-epi-25-hydroxyvitamin D3 (50 ug/mL), 1,25-dihydroxyvitamin D3 (10 ug/mL), and [$^{13}C_5$]- 1,25-dihydroxyvitamin D3 (10 ug/mL), 24R,25-dihydroxyvitamin D3 (100 ug/mL), d_6-24R,25-dihydroxyvitamin D3 (100 ug/mL), and [$^{13}C_5$]-24R,25-dihydroxyvitamin D3 (50 ug/mL). Structures for labeled isotopologues are included in the Supporting Information to show the precise location of the heavy labels (Figure S1). Standards of Vitamin D2 and D3 were also purchased from Cayman Chemical (Ann Arbor, MI) as 1 mg/mL solutions in acetonitrile. All solvents used (water (0.1% formic acid), methanol, and acetonitrile) were Fisher Scientific Optima LC-MS grade.

Sample Preparation

Working solutions of all Vitamin D metabolites were prepared individually or as mixtures (of isomers and/or isotopologues) in 50% (v/v) aqueous methanol at concentrations ranging from 100-1000 ng/mL, as indicated.

Instrumentation

All analyses were first performed in triplicate using an Agilent 6560 drift tube (DT) IM-QTOF (Santa Clara, CA) for direct measurement of collision cross section (CCS). Samples were introduced via direct injection (10 µL) with a flow rate of 0.300 mL/min of (50:50 (v/v) water (0.1% formic acid)/methanol) using an Agilent 1290 Infinity II UHPLC. Ionization was performed with an Agilent Jetstream (AJS) ESI source in positive mode, and the MS data were acquired using full scan mode. The drift tube was maintained at approx. 3.95 Torr nitrogen and approx. 27 °C, and the electric field strength was 18.5 V/cm. CCS values were measured using the established single-field method[15] based on beta and t-fix values for the Agilent Tune Mix ions. Further instrument parameters can be found in the Supporting Information (Table S2).

Analyses were also performed in triplicate using a MOBIE HRIM SLIM (MOBILion Systems, Inc., Chadd's Ford, PA) coupled to an Agilent 6546 QTOF (Santa Clara, CA). Samples were introduced via direct injection (10 µL) with a flow rate of 0.300 mL/min of (50:50 (v/v) water (0.1% formic acid)/methanol) using an Agilent 1290 Infinity II UHPLC. Ionization was performed with an Agilent Jetstream (AJS) ESI source in positive mode. The SLIM device was maintained at 2.50 Torr nitrogen gas and 25 °C. SLIM traveling wave (TW) parameters were first optimized in short path (0.4 m) IM mode, and then separations and analysis were performed using HRIM (13 m) mode. Briefly, these conditions included a 100 ms trapping time and SLIM TW operated at 35 kHz frequency and 45 V_{pp} amplitude; based on the electrode geometry, this frequency equates to a TW speed of 315 m/s. Further details of the SLIM and QTOF parameters can be found in the Supporting Information (Table S3).

Data Processing and Analysis

Acquisition of the IM-QTOF data was performed using Agilent MassHunter B.09.00 (Build 9.0.9044.0) and visualized/processed in Agilent IM-MS Browser 10.0.1 (Build 10.0.1.10039). SLIM data acquisition was performed using Agilent MassHunter Acquisition Version 11.0 (Build

11.0.221.1) and MOBILion EyeOn software (0.0.2.2619-release-1.5.14.3). All SLIM data was first converted from the MOBILion .mbi file format into Agilent .d file format using the EyeOn software, and then pre-processed using the PNNL PreProcessor 4.0 (2022.02.18) (Richland, WA) with a drift bin compression of 3:1 and CCS conversion.[49] Further data visualization/processing was then performed using Agilent IM-MS Browser 10.0.1 (Build 10.0.1.10039). Selected SLIM HRIM data was manually fitted to gaussian peaks, as indicated. CCS measurements were made by first calibrating the SLIM system using the Agilent Tune Mix ions, which allowed for conversion of arrival time to CCS using the PNNL PreProcessor.[32,49] Briefly, this calibration process involved plotting of experimental arrival times for the Agilent Tune Mix ions (acquired using experimental parameters identical to those used for measurement of the vitamin D compounds) against their corresponding reduced $^{DT}CCS_{N2}$ values, which allowed for creation of a third order polynomial calibration curve. Experimental arrival times for the vitamin D metabolites could then be converted into reduced CCS and then (using charge and reduced mass) into conventional $^{SLIM}CCS_{N2}$. Further details of this calibration process are found in a recent paper by Rose et al.[32]

For comparison of mass distribution-based (i.e., isotopic) mobility shifts, relative arrival times were calculated by first fitting raw arrival time data to a Gaussian curve (at 50% peak height), as proposed by Williamson et al.[41] Peak apexes from the fitted Gaussians were then used for calculating error and for comparison of relative arrival times.

RESULTS AND DISCUSSION

Measurement of SLIM-Based Collision Cross Section (CCS)

In total, 14 different vitamin D metabolites and their isotopologues were measured with both low-resolution drift tube IM and high-resolution SLIM IM. SLIM traveling wave (TW) conditions were optimized (frequency and amplitude) for resolving power and signal abundance, by systematically ramping frequency or amplitude while keeping the other parameter constant; this yielded optimized TW conditions of 45 V and 35,000 Hz (Figure S1). SLIM CCS measurements required calibration using the Agilent Tune Mix, as previously, using these specifically optimized TW conditions.[32,34] Unlike in those previous studies, where SLIM demonstrated minor, yet easily correctable, $^{SLIM}CCS_{N2}$ bias (roughly ~2-3% positive bias for lipids[32] and ~1% negative bias for synthetic cannabinoid metabolites[34]), these values differed from their matching $^{DT}CCS_{N2}$ (Table S4) by an average of <0.1% (Table 1); all values agreed with their corresponding $^{DT}CCS_{N2}$ values to within ±0.5%, with the only exception being a previously unresolved peak that will be discussed later. Additionally, the standard deviation of replicate measurements was ±0.2 $Å^2$ for nearly all compounds. This demonstrates both the accuracy and precision of the SLIM technique for CCS measurements.

Table 1. $^{SLIM}CCS_{N2}$ measurement of vitamin metabolites and their isotopologues, including associated chemical formula/theoretical mass and difference from measured $^{DT}SLIM_{N2}$ values, reported as %ΔCCS. *New peaks only identified by SLIM are marked with an asterisk.

Compound	Formula	$[M+Na]^+$ *m/z*	$^{SLIM}CCS_{N2}$ (Å^2)	%ΔCCS
25-Hydroxyvitamin D3	$C_{27}H_{44}O_2$	423.3239	204.6 ± 0.1	-0.10%
			232.2 ± 0.1	-0.01%
25-Hydroxyvitamin D3-[$^{13}C_5$]	$C_{22}{}^{13}C_5H_{44}O_2$	428.3407	204.7 ± 0.2	-0.10%
			232.4 ± 0.1	0.08%
3-epi-25-Hydroxyvitamin D3	$C_{27}H_{44}O_2$	423.3239	202.8 ± 0.1*	-0.10%*
			204.2 ± 0.1*	0.54%*
3-epi-25-Hydroxyvitamin D3-[$^{13}C_5$]	$C_{22}{}^{13}C_5H_{44}O_2$	428.3407	202.8 ± 0.1*	-0.18%*
			204.3 ± 0.1*	0.56%*
Vitamin D3-[d_3]	$C_{27}H_{41}D_3O$	410.3478	ND	
			ND	
1,25-Dihydroxyvitamin D3-[$^{13}C_5$]	$C_{22}{}^{13}C_5H_{44}O_3$	444.3356	207.1 ± 0.1*	-0.77%*
			208.7 ± 0.1*	0.00%*
24,25-Dihydroxyvitamin D3	$C_{27}H_{44}O_3$	439.3188	207.8 ± 0.1	-0.50%
			241.9 ± 0.1	-0.47%
24,25-Dihydroxyvitamin D3-[$^{13}C_5$]	$C_{22}{}^{13}C_5H_{44}O_3$	444.3356	208.0 ± 0.1	-0.49%
			242.0 ± 0.1	-0.47%
24,25-Dihydroxyvitamin D3-[d_6]	$C_{27}H_{38}D_6O_3$	445.3565	208.0 ± 0.1	-0.51%
			241.9 ± 0.1	-0.53%
25-Hydroxyvitamin D2	$C_{28}H_{44}O_2$	435.3240	208.8 ± 0.7	-0.31%
			231.2 ± 0.1	0.08%
25-Hydroxyvitamin D2-[$^{13}C_5$]	$C_{23}{}^{13}C_5H_{44}O_2$	440.3407	209.0 ± 0.1	-0.34%
			231.3 ± 0.1	0.08%
Epi-25-Hydroxyvitamin D2-[$^{13}C_5$]	$C_{23}{}^{13}C_5H_{44}O_2$	440.3407	204.7 ± 0.1	-0.21%*
			208.4 ± 0.1	1.59%*
Vitamin D2-[d_3]	$C_{28}H_{41}D_3O$	422.3478	217.7 ± 0.7	-0.04%
			230.5 ± 0.1	0.03%
1,25-Dihydroxyvitamin D2-[$^{13}C_5$]	$C_{23}{}^{13}C_5H_{44}O_3$	456.3356	211.3 ± 0.1	-0.08%

SLIM IM Separations of Isomers and Identification of New Conformers

We principally investigated the ion mobility patterns and separation of three isomers groups: 25-hydroxyvitamin D3 (25OHD3) and its epimer (epi25OHD3); 25-hydroxyvitamin D2 (25OHD2) and its epimer (epi25OHD2); and 1,25-dihydroxyvitamin D3 (1,25-DiOHD3) and its structural isomer 24,25-dihydroxyvitamin D3 (24,24-DiOHD3). The SLIM IM overlay for 25OHD3/epi25OHD3 is shown in Figure 1A and largely resembles the pattern observed with DTIMS (Figure S2A), with overlapping peaks at CCS ~205 Å^2 and the unique 'open' conformer for 25OHD3 at $^{SLIM}CCS_{N2}$ 232.2 Å^2. However, looking more closely at the pattern for the 'closed' conformer revealed the presence of a second mobility peak for epi25OHD3 (Figure 1B). It should be noted that the peak width measured by DTIMS (Figure 1C) for this compound is slightly larger than expected based on typical resolving power for this instrument (R_p ~50-60); the measured resolving power based on this peak would yield R_p ~40, and this observation alone could be used as the basis for multiple conformers thereunder. While the lower mobility peak (CCS 204.2 Å^2) is unresolved from the 'closed' conformer of 25OHD3, the higher mobility species (CCS 202.8 Å^2), presumably a similar 'closed' conformer, is well separated from 25OHD3 and could thus be used to differentiate and potentially quantify; a previous conformational search indicated several possible 'closed' structures for epi25OHD3, all within an energetically accessible range, which presumably gives rise to the newly observed species.[16] It should be noted that two peaks for epi25OHD3 were also previously identified by Oranzi et al.,[19] where TIMS analysis partially resolved two species and FAIMS fully resolved these species.

There have been fewer studies on the structural/conformational preferences of 25-hydroxyvitamin D2 (the plant derived compound), but DTIMS work by Chouinard et al. showed a similar pattern of multiple mobility peaks, again 'open' and 'closed' conformations confirmed by computational modeling.[16] The sole mobility peak for the epimer partially overlapped with the 'closed' conformation of 25OHD2, precluding resolution. Our current SLIM work demonstrates the

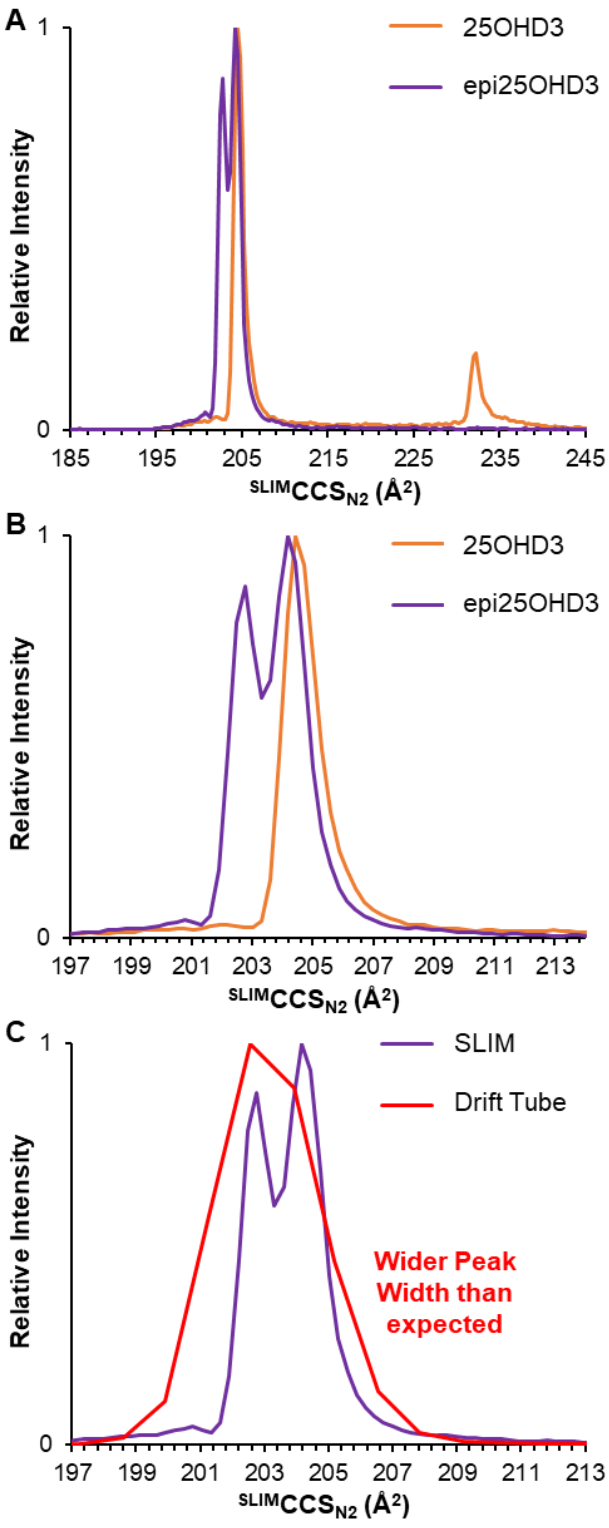

Figure 1. SLIM-based ion mobility separations of 25-hydroxyvitamin D3 (25OHD3) and epi-25-hydroxyvitamin D3 (epi25OHD3) showing (A) the multiple conformations observed and (B) a zoomed spectrum with the newly observed mobility feature for epi25OHD3. (C) This new feature can be inferred from the wider peak width seen when analyzed by low-resolution DTIMS.

repeatable conformational pattern for 25OHD2 (Figure 2A), but interestingly a second mobility peak is observed for the epimer (Figure 2B). While these isomers are unresolved by DTIMS (Figure S2B), closer investigation does seem to indicate the presence of a shoulder on the epi25OHD2 mobility peak. The higher resolving power of SLIM shows that this shoulder is indeed due to a second, presumably also 'closed', conformation; these two species have measured $^{SLIM}CCS_{N2}$ of 204.7 and 208.4 Å^2, a difference of only ~1.8% which is not resolvable by DTIMS but shows the value of SLIM (Figure 2C). But, most importantly, the higher mobility species ($^{SLIM}CCS_{N2}$ 204.7 Å^2) is baseline resolved from the 'closed' conformer of 25OHD2. Based on this species and the 'open' conformer of 25OHD2, these two epimers can now be completely resolved and this provides the potential for future quantification.

Unlike 25OHD3/25OHD2 and their epimers, 1,25-dihydroxyvitamin D3 (calcitriol) is the active form of vitamin D which is tested for clinical to evaluate for hypercalcemia and renal failure. But this compound similarly has an endogenous isomer, 24,25-dihydroxyvitamin D3, which is another inactive metabolite and thus is important to differentiate. This isomer displayed a pattern similar to 25OHD3/25OHD2 with two well resolved mobility features (Figure 3A), but the higher mobility feature partially overlaps with calcitriol which shows two moderately resolved peaks at $^{SLIM}CCS_{N2}$ of 207.0 and 208.7 Å^2, a difference of only 0.8% (Figure 3B). But what is most interesting about this compound is that, unlike for both epi25OHD3 and 25OHD2, the DTIMS results (Figure 3C) show no obvious indication of multiple conformers. This is another example of the benefit of using high-resolution ion mobility. Importantly, the lower mobility feature ($^{SLIM}CCS_{N2}$ 208.7 Å^2) is partially resolved from 24,25-dihydroxyvitamin D3 and could be used as a unique diagnostic mobility.

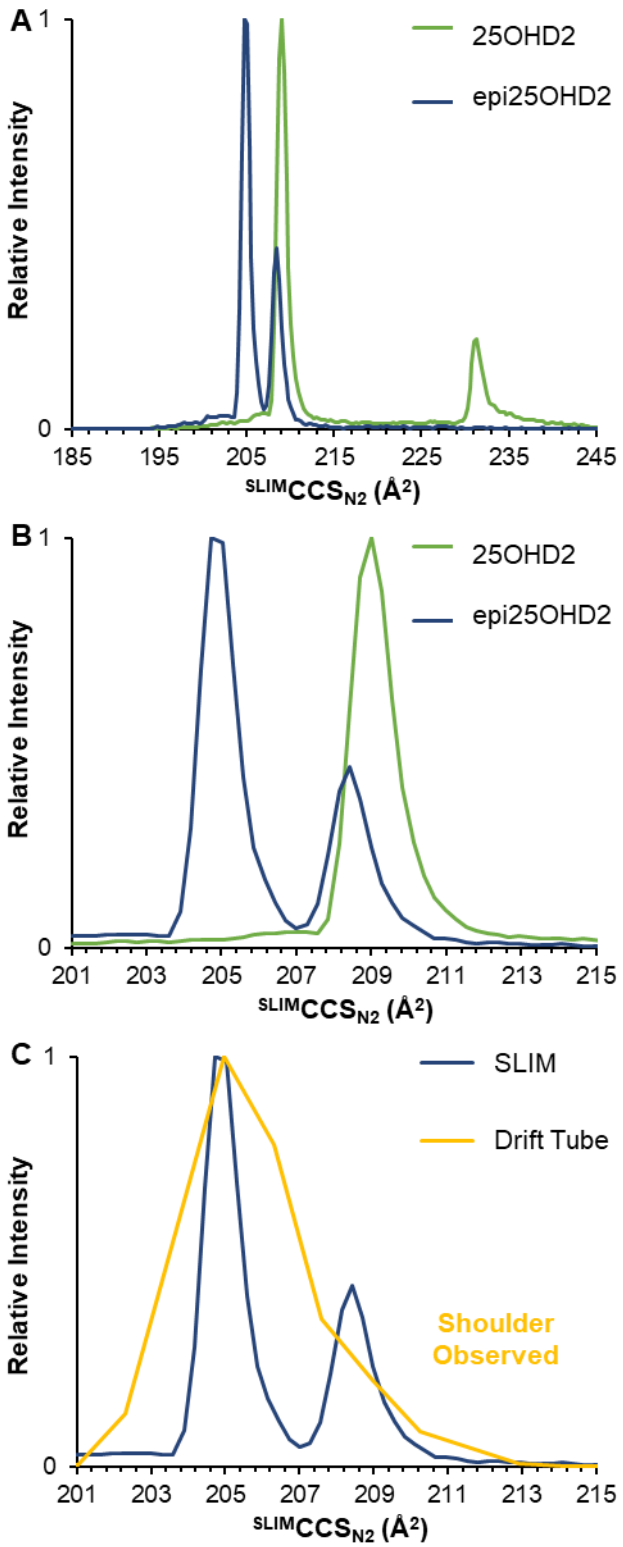

Figure 2. SLIM-based ion mobility separations of 25-hydroxyvitamin D2 (25OHD2) and epi-25-hydroxyvitamin D2 (epi25OHD2) showing (A) the multiple conformations observed and (B) a zoomed spectrum with the newly observed mobility feature for epi25OHD2. (C) This new feature can be inferred from the shoulder observed when analyzed by low-resolution DTIMS.

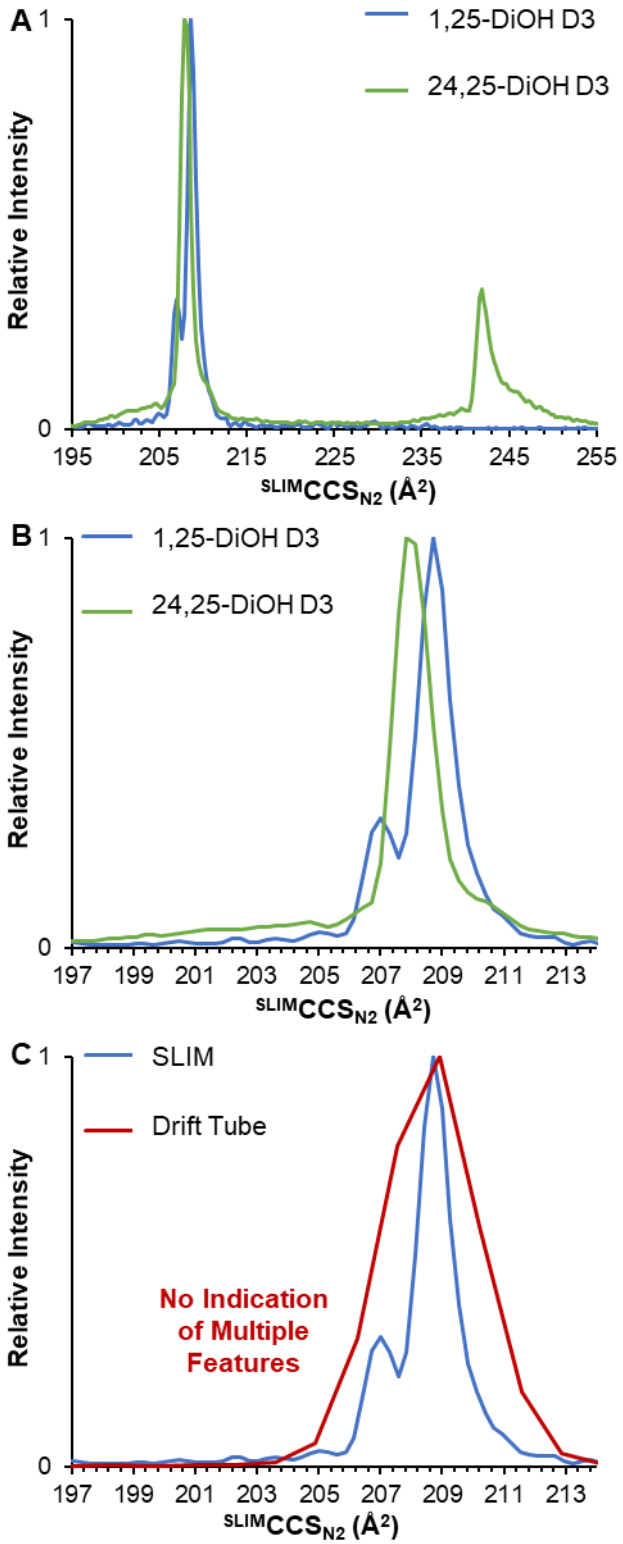

Figure 3. SLIM-based ion mobility separations of 1,25-hydroxyvitamin D3 (1,25-DiOH D3) and 24,25-hydroxyvitamin D3 (24,25-DiOH D3) showing (A) the multiple conformations observed and (B) a zoomed spectrum with the newly observed mobility feature for 1,25-DiOH D3. (C) This new feature cannot be inferred solely from the low-resolution DTIMS results.

Measurement of Mobility Shifts Due to Isotopic Labeling

This sample set of isotopologues provided a unique opportunity to expand upon previous work by Williamson et al. investigating mass distribution-based mobility shifts.[41] First, a mixture of 25OHD3 and 25OHD3-$^{13}C_5$ were measured in triplicate and their arrival time distributions fitted to a Gaussian (at 50% peak height). We investigated the effects of ^{13}C- and/or deuterium-labeling on relative arrival time and calculation of $\Delta^{SLIM}CCS_{N2}$, as relative arrival time and ΔCCS have been demonstrated to have much higher precision as compared to measurement of arrival time or raw CCS for a single ion.[37,41,48] Those Gaussian peak apexes were compared for both the 'closed' and 'open' conformations (Figure 4A-B, respectively). We observed a +0.21% increase in arrival time for the 'closed' conformer of the labeled version, and a +0.33% increase for the 'open' conformer. The 25OHD3-$^{13}C_5$ isotopologue would be anticipated to shift in arrival time based on reduced mass, but reduced mass only differs by ~0.07% and so these larger shifts indicate the likelihood of effects due to center of mass/moment of inertia. While these relative shifts cannot be directly compared to the cIMS results from Williamson et al., due to significant differences in the instrumentation (i.e., cyclic vs. serpentine path, different traveling wave conditions, etc.) and path length, the same general trend of a larger relative shift (by ~50%) for the extended 'open' conformation relative to the compact 'closed' conformation is observed and largely correlates well with those previous results. Matching CCS-converted plots are shown in Figure 4C-D, however the conversion process from raw arrival time to CCS involves factoring in reduced mass (via reduced CCS, as proposed by Rose et al.[32]) and so the shift that is still observed is clearly due to non-mass distribution effects (i.e., center of mass/moment of inertia). It should be noted that all plots shown in Figure 4 show raw data, but the actual relative arrival time shifts or CCS values were based on peak apexes determined from Gaussian fitting as has been suggested previously (shown in Figure S3).[41]

Aside from the fundamental interest in these mass-based mobility shifts, from a quantitative standpoint it is imperative to measure and understand the magnitude of such shifts

to allow for appropriate arrival time- or CCS-based extraction prior to peak area integration being used for absolute quantitation. This consideration is analogous to the need to appropriately account for minor chromatographic retention shift for highly deuterium-labeled internal standards. To assess the magnitude of error that would be associated with using 25OHD3-$^{13}C_5$, we compared integrated peak areas over an arrival time range based on bounds established for the unlabeled compound. This yielded (for the 'closed' conformer) a difference in peak area of ~5.4%, which would proportionately affect any concentration values calculated based on this internal standard. However, understanding this highly repeatable shift for any given isotopically labeled standard in comparison with its unlabeled endogenous counterpart would allow this effect to be accounted for to provide accurate quantitative values.

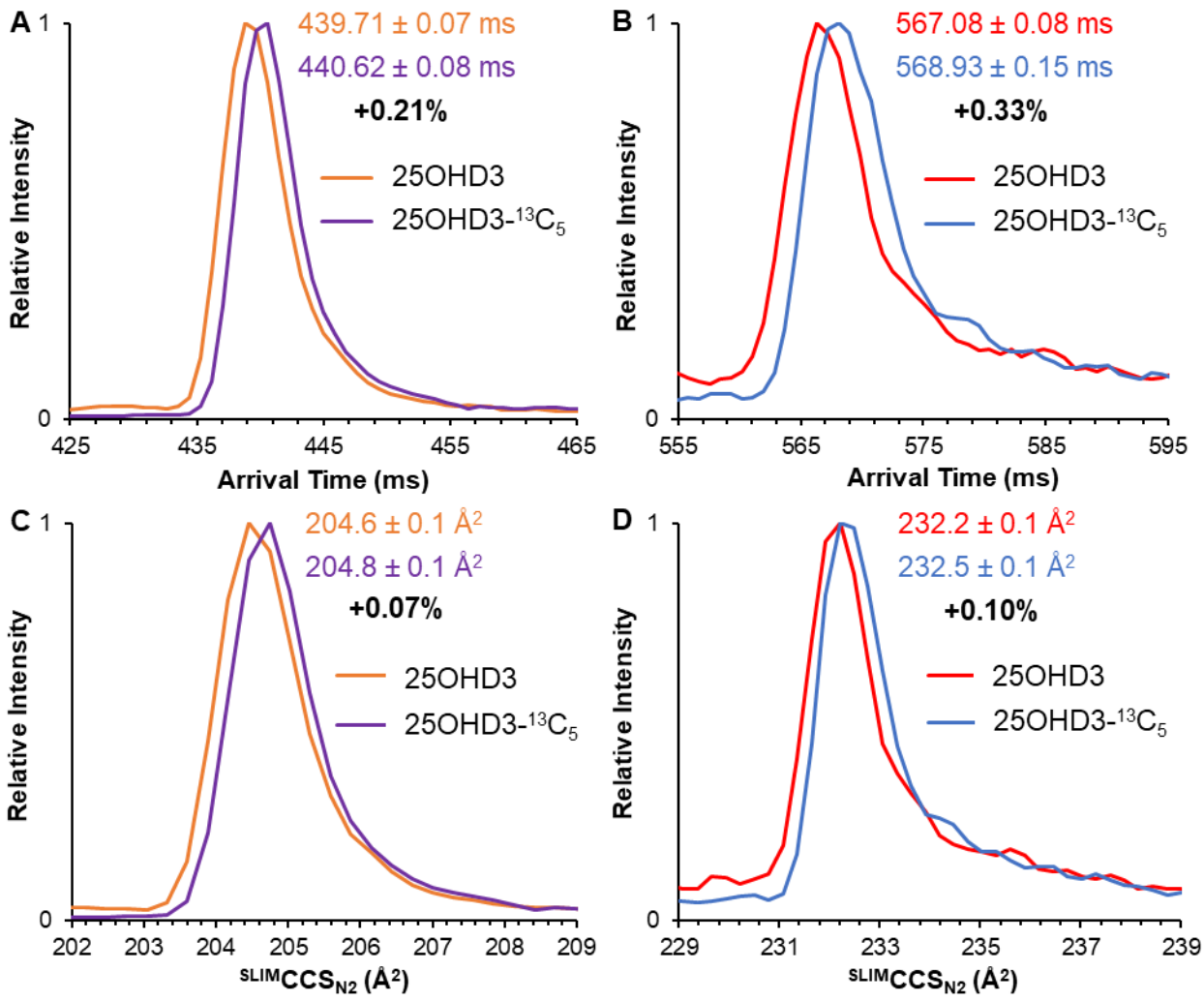

Figure 4. SLIM-based ion mobility separations of 25OHD3 and 25OHD3-$^{13}C_5$ for both (A) the compact 'closed' conformer and (B) the extended 'open' conformer. Gaussian fitted arrival times, measurement error, and difference between the isotopologues are indicated. (C-D) CCS converted plots are also shown, with Gaussian fitted CCS, measurement error, and the difference between the isotopologues indicated to show the non-mass distribution effects.

Lastly, we investigated how different isotopologues, specifically ^{13}C- vs. deuterium-labeled versions, would differ in their arrival time distribution. Figure 5 shows raw arrival time distributions for 24,25-dihydroxyvitamin D3 and its $^{13}C_5$- and d_6-labeled isotopologues for both the 'closed' (Figure 5A) and 'open' conformers (Figure 5B). Both of these isotopologues are labeled in similar locations towards the terminal end of the molecule (Table S1). The relative arrival time shifts (as determined from a Gaussian fit of the raw data) for $^{13}C_5$- and d_6-labeled versions of the 'closed' conformer were only 0.21% and 0.24%, respectively, and 0.23% and 0.18% for the 'open' conformer; however, these values are all within the relative arrival time error associated with the triplicate measurements made and given the resolving power of this instrument it is not possible to confidently differentiate the isotopic shifts between these isotopologues. The converted CCS values (again, as determined from a Gaussian fit of the raw data), which account for differences in reduced mass between the isotopologues, for $^{13}C_5$- and d_6-labeled versions of the 'closed' conformer were only 0.08% and 0.08% higher, respectively, and 0.05% and 0.02% for the 'open' conformer. These differences indicate the contribution from non-mass distribution effects (i.e., center of mass/moment of inertia). Most importantly, while both isotopologues are shifted relative to the unlabeled endogenous version, because of the similarity in the label position (thus not contributing significantly to relative differences in center of mass) the shifts are very similar. This concludes that, as long as their shifts are accounted for, both ^{13}C- and d-labeled can be used as internal standards for the analysis of endogenous vitamin D metabolites with high resolution IM.

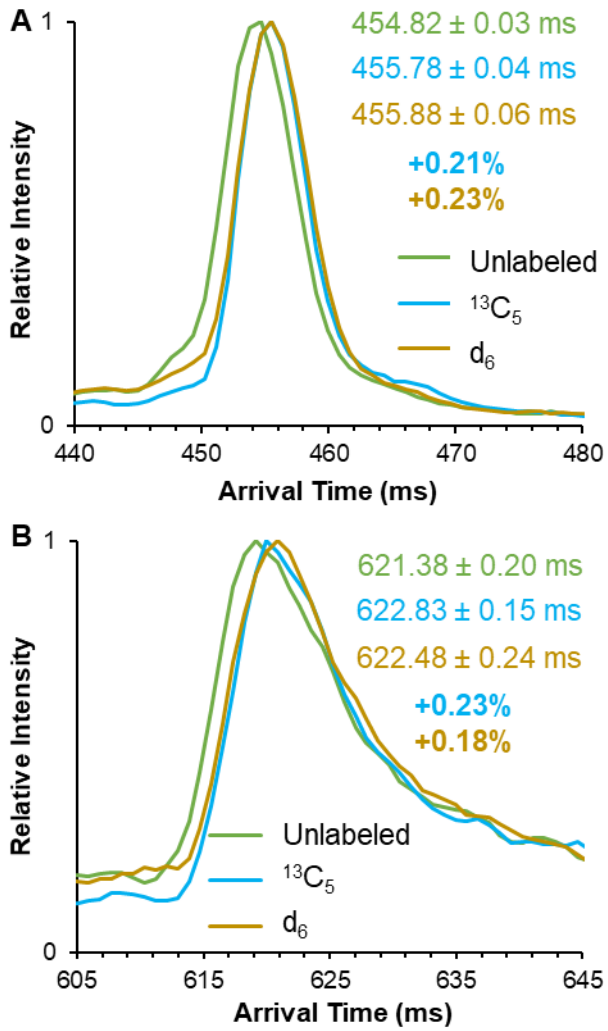

Figure 5. SLIM-based ion mobility separations of unlabeled 24,24-dihydroxyvitamin D3 and its $^{13}C_5$- and d_6-labeled isotopologues for both (A) the compact 'closed' conformer and (B) the extended 'open' conformer.

CONCLUSION

In this study, we investigated the high-resolution SLIM ion mobility pattern of 14 vitamin D metabolite isomers and isotopologues. Measured $^{SLIM}CCS_{N2}$ and $^{DT}CCS_{N2}$ values were in strong agreement, differing on average by an average of <0.1%. Interestingly, the high resolving power of SLIM revealed new ion mobility peaks for the 'closed' conformer of epi25OHD3, epi25OHD2, and 1,25-dihydroxyvitamin D3, where low-resolution drift tube IMS was not able to confidently

differentiate such species. These new mobility features especially provided a unique CCS that could be used to differentiate the isomers and holds tremendous promise for future quantitative applications. As another critical consideration in quantification, the mobility shifts of isotopically labeled standards (^{13}C and/or deuterium-labeled) were assessed and showed minor (yet important) changes in arrival time distribution of roughly 0.2-0.3%. Appropriately accounting for these shifts will reduce introduction of error into data extraction and peak area integration for future targeted analysis. Overall, this SLIM-based analysis of vitamin D metabolites holds significant potential as a rapid, high-throughput method for excellent prospects for clinical analysis. Future studies will incorporate a fast (≤2 min) chromatographic separation for absolute quantification of these metabolite D metabolites in human serum.

ASSOCIATED CONTENT

Supporting Information. The Supporting Information is available free of charge. Structures of isotopologues; IM-MS instrumental parameters; $^{DT}CCS_{N2}$ values for all metabolites/isotopologues; optimization of SLIM TW conditions; DTIMS overlays; and Gaussian fitted SLIM data.

AUTHOR INFORMATION

Corresponding Author

*Email: cchouin@clemson.edu

Author Contributions

SK, MH, TPB, and ARS prepared and analyzed the samples. SK and CDC processed the data and wrote the manuscript. All authors have given approval to the final version of the manuscript.

Notes

The authors declare no competing financial interests.

ACKNOWLEDGMENTS

The authors would like to thank Rich Tyburski and Steve Jones from Advanced Stable Isotope (ASI) Chemicals for their numerous contributions to this research. We would also like to acknowledge Gabe Nagy (University of Utah) for quite helpful discussions of isotopologue separations. Financial support for this work was provided by Agilent Technologies (Global Academic Research Support Program #2624930) and Clemson University startup funds. Authors acknowledge the financial support from NSF, Division of Chemistry, Award CHE-2050042. Special thanks to Carlos Garcia, Bill Pennington, and Tania Houjeiry for their role in the Clemson Chemistry REU program that provided Selena Kingsley the opportunity to perform this research.

REFERENCES

(1) Lips, P. Vitamin D Physiology. *Progress in Biophysics and Molecular Biology*. September 2006, pp 4–8. https://doi.org/10.1016/j.pbiomolbio.2006.02.016.

(2) Mayo Clinic Staff. *Vitamin D*. https://www.mayoclinic.org/drugs-supplements-vitamin-d/art-20363792.

(3) Holick, M. F.; Binkley, N. C.; Bischoff-Ferrari, H. A.; Gordon, C. M.; Hanley, D. A.; Heaney, R. P.; Murad, M. H.; Weaver, C. M. Evaluation, Treatment, and Prevention of Vitamin D Deficiency: An Endocrine Society Clinical Practice Guideline. *Journal of Clinical Endocrinology and Metabolism*. July 1, 2011, pp 1911–1930. https://doi.org/10.1210/jc.2011-0385.

(4) Máčová, L.; Bičíková, M. Vitamin d: Current Challenges between the Laboratory and Clinical Practice. *Nutrients*. MDPI AG June 1, 2021. https://doi.org/10.3390/nu13061758.

(5) D. Carter, G. Accuracy of 25-Hydroxyvitamin D Assays: Confronting the Issues. *Curr Drug Targets* **2011**, *12* (1), 19–28. https://doi.org/10.2174/138945011793591608.

(6) Binkley, N.; Krueger, D.; Cowgill, C. S.; Plum, L.; Lake, E.; Hansen, K. E.; DeLuca, H. F.; Drezner, M. K. Assay Variation Confounds the Diagnosis of Hypovitaminosis D: A Call for Standardization. *J Clin Endocrinol Metab* **2004**, *89* (7), 3152–3157. https://doi.org/10.1210/jc.2003-031979.

(7) Kaufmann, M.; Gallagher, J. C.; Peacock, M.; Schlingmann, K. P.; Konrad, M.; DeLuca, H. F.; Sigueiro, R.; Lopez, B.; Mourino, A.; Maestro, M.; St-Arnaud, R.; Finkelstein, J. S.; Cooper, D. P.; Jones, G. Clinical Utility of Simultaneous Quantitation of 25-Hydroxyvitamin D and 24,25-Dihydroxyvitamin D by LC-MS/MS Involving Derivatization with DMEQ-TAD. *Journal of Clinical Endocrinology and Metabolism* **2014**, *99* (7), 2567–2574. https://doi.org/10.1210/jc.2013-4388.

(8) Zelzer, S.; Goessler, W.; Herrmann, M. Measurement of Vitamin D Metabolites by Mass Spectrometry, an Analytical Challenge. *J Lab Precis Med* **2018**, *3*, 99–99. https://doi.org/10.21037/jlpm.2018.11.06.

(9) Volmer, D. A.; Mendes, L. R. B. C.; Stokes, C. S. Analysis of Vitamin D Metabolic Markers by Mass Spectrometry: Current Techniques, Limitations of the “Gold Standard” Method, and Anticipated Future Directions. *Mass Spectrom Rev* **2015**, *34* (1), 2–23. https://doi.org/10.1002/mas.21408.

(10) Qi, Y.; Geib, T.; Schorr, P.; Meier, F.; Volmer, D. A. On the Isobaric Space of 25-Hydroxyvitamin D in Human Serum: Potential for Interferences in Liquid Chromatography/Tandem Mass Spectrometry, Systematic Errors and Accuracy Issues. *Rapid Communications in Mass Spectrometry* **2014**, *29* (1), 1–9. https://doi.org/10.1002/rcm.7075.

(11) Volmer, D. A.; Stokes, C. S. Analytical Considerations for Accurately Capturing the Relevant Species Contributing to Vitamin D Status in Liquid Chromatography-Tandem Mass Spectrometry Assays. *Analytical Science Advances* **2022**, *3* (1–2), 14–20. https://doi.org/10.1002/ansa.202100057.

(12) Chouinard, C. D.; Wei, M. S.; Beekman, C. R.; Kemperman, R. H. J.; Yost, R. A. Ion Mobility in Clinical Analysis: Current Progress and Future Perspectives. *Clinical Chemistry*. American Association for Clinical Chemistry Inc. January 1, 2016, pp 124–133. https://doi.org/10.1373/clinchem.2015.238840.

(13) Koomen, D. C.; May, J. C.; McLean, J. A. Insights and Prospects for Ion Mobility-Mass Spectrometry in Clinical Chemistry. *Expert Rev Proteomics* **2022**, *19* (1), 17–31. https://doi.org/10.1080/14789450.2022.2026218.

(14) Dodds, J. N.; Baker, E. S. Ion Mobility Spectrometry: Fundamental Concepts, Instrumentation, Applications, and the Road Ahead. *J Am Soc Mass Spectrom* **2019**, *30* (11), 2185–2195. https://doi.org/10.1007/s13361-019-02288-2.

(15) Kobold, U.; Thiele, R.; Weiss, N.; Brown, L. Method and Device for Separating Metabolites or Stereoisomers, 2017. https://patents.google.com/patent/WO2015185487A1/en

(16) Chouinard, C. D.; Cruzeiro, V. W. D.; Beekman, C. R.; Roitberg, A. E.; Yost, R. A. Investigating Differences in Gas-Phase Conformations of 25-Hydroxyvitamin D3 Sodiated Epimers Using Ion Mobility-Mass Spectrometry and Theoretical Modeling. *J Am Soc Mass Spectrom* **2017**, *28* (8), 1497–1505. https://doi.org/10.1007/s13361-017-1673-4.

(17) Chouinard, C. D.; Cruzeiro, V. W. D.; Kemperman, R. H. J.; Oranzi, N. R.; Roitberg, A. E.; Yost, R. A. Cation-Dependent Conformations in 25-Hydroxyvitamin D3-Cation Adducts Measured by Ion Mobility-Mass Spectrometry and Theoretical Modeling. *Int J Mass Spectrom* **2018**, *432*, 1–8. https://doi.org/10.1016/j.ijms.2018.05.013.

(18) Oranzi, N. R.; Polfer, N. C.; Lei, J.; Yost, R. A. Influence of Experimental Conditions on the Ratio of 25-Hydroxyvitamin D3 Conformers for Validating a Liquid Chromatography/Ion Mobility-Mass Spectrometry Method for Routine Quantitation. *Anal Chem* **2018**, *90* (22), 13549–13556. https://doi.org/10.1021/acs.analchem.8b03668.

(19) Oranzi, N. R.; Kemperman, R. H. J.; Wei, M. S.; Petkovska, V. I.; Granato, S. W.; Rochon, B.; Kaszycki, J.; La Rotta, A.; Jeanne Dit Fouque, K.; Fernandez-Lima, F.; Yost, R. A. Measuring the Integrity of Gas-Phase Conformers of Sodiated 25-Hydroxyvitamin D3 by Drift Tube, Traveling Wave, Trapped, and High-Field Asymmetric Ion Mobility. *Anal Chem* **2019**, *91* (6), 4092–4099. https://doi.org/10.1021/acs.analchem.8b05723.

(20) Oranzi, N. R.; Lei, J.; Kemperman, R. H. J.; Chouinard, C. D.; Holmquist, B.; Garrett, T. J.; Yost, R. A. Rapid Quantitation of 25-Hydroxyvitamin D2 and D3 in

Human Serum Using Liquid Chromatography/Drift Tube Ion Mobility-Mass Spectrometry. *Anal Chem* **2019**, *91* (21), 13555–13561. https://doi.org/10.1021/acs.analchem.9b02683.

(21) Usoltseva, L.; Ioutsi, V.; Panov, Y.; Antsupova, M.; Rozhinskaya, L.; Melnichenko, G.; Mokrysheva, N. Serum Vitamin D Metabolites by HPLC-MS/MS Combined with Differential Ion Mobility Spectrometry: Aspects of Sample Preparation without Derivatization. *Int J Mol Sci* **2023**, *24* (9). https://doi.org/10.3390/ijms24098111.

(22) Chai, Y.; Grebe, S. K. G.; Maus, A. Improving LC-MS/MS Measurements of Steroids with Differential Mobility Spectrometry. *Journal of Mass Spectrometry and Advances in the Clinical Lab* **2023**, *30*, 30–37. https://doi.org/10.1016/j.jmsacl.2023.10.001.

(23) Webb, I. K.; Garimella, S. V. B.; Tolmachev, A. V.; Chen, T. C.; Zhang, X.; Norheim, R. V.; Prost, S. A.; LaMarche, B.; Anderson, G. A.; Ibrahim, Y. M.; Smith, R. D. Experimental Evaluation and Optimization of Structures for Lossless Ion Manipulations for Ion Mobility Spectrometry with Time-of-Flight Mass Spectrometry. *Anal Chem* **2014**, *86* (18), 9169–9176. https://doi.org/10.1021/ac502055e.

(24) Hamid, A. M.; Ibrahim, Y. M.; Garimella, S. V. B.; Webb, I. K.; Deng, L.; Chen, T. C.; Anderson, G. A.; Prost, S. A.; Norheim, R. V.; Tolmachev, A. V.; Smith, R. D. Characterization of Traveling Wave Ion Mobility Separations in Structures for Lossless Ion Manipulations. *Anal Chem* **2015**, *87* (22), 11301–11308. https://doi.org/10.1021/acs.analchem.5b02481.

(25) Deng, L.; Ibrahim, Y. M.; Baker, E. S.; Aly, N. A.; Hamid, A. M.; Zhang, X.; Zheng, X.; Garimella, S. V. B.; Webb, I. K.; Prost, S. A.; Sandoval, J. A.; Norheim, R. V.; Anderson, G. A.; Tolmachev, A. V.; Smith, R. D. Ion Mobility Separations of Isomers Based upon Long Path Length Structures for Lossless Ion Manipulations Combined with Mass Spectrometry. *ChemistrySelect* **2016**, *1* (10), 2396–2399. https://doi.org/10.1002/slct.201600460.

(26) Ibrahim, Y. M.; Hamid, A. M.; Deng, L.; Garimella, S. V. B.; Webb, I. K.; Baker, E. S.; Smith, R. D. New Frontiers for Mass Spectrometry Based upon Structures for Lossless Ion Manipulations. *Analyst*. Royal Society of Chemistry April 7, 2017, pp 1010–1021. https://doi.org/10.1039/c7an00031f.

(27) Deng, L.; Webb, I. K.; Garimella, S. V. B.; Hamid, A. M.; Zheng, X.; Norheim, R. V.; Prost, S. A.; Anderson, G. A.; Sandoval, J. A.; Baker, E. S.; Ibrahim, Y. M.; Smith, R. D. Serpentine Ultralong Path with Extended Routing (SUPER) High Resolution Traveling Wave Ion Mobility-MS Using Structures for Lossless Ion Manipulations. *Anal Chem* **2017**, *89* (8), 4628–4634. https://doi.org/10.1021/acs.analchem.7b00185.

(28) Nagy, G.; Attah, I. K.; Garimella, S. V. B.; Tang, K.; Ibrahim, Y. M.; Baker, E. S.; Smith, R. D. Unraveling the Isomeric Heterogeneity of Glycans: Ion Mobility Separations in Structures for Lossless Ion Manipulations. *Chemical*

Communications **2018**, *54* (83), 11701–11704. https://doi.org/10.1039/c8cc06966b.

(29) Nagy, G.; Chouinard, C. D.; Attah, I. K.; Webb, I. K.; Garimella, S. V. B.; Ibrahim, Y. M.; Baker, E. S.; Smith, R. D. Distinguishing Enantiomeric Amino Acids with Chiral Cyclodextrin Adducts and Structures for Lossless Ion Manipulations. *Electrophoresis* **2018**, *39* (24), 3148–3155. https://doi.org/10.1002/elps.201800294.

(30) Chouinard, C. D.; Nagy, G.; Webb, I. K.; Shi, T.; Baker, E. S.; Prost, S. A.; Liu, T.; Ibrahim, Y. M.; Smith, R. D. Improved Sensitivity and Separations for Phosphopeptides Using Online Liquid Chromotography Coupled with Structures for Lossless Ion Manipulations Ion Mobility-Mass Spectrometry. *Anal Chem* **2018**, *90* (18), 10889–10896. https://doi.org/10.1021/acs.analchem.8b02397.

(31) Chouinard, C. D.; Nagy, G.; Webb, I. K.; Garimella, S. V. B.; Baker, E. S.; Ibrahim, Y. M.; Smith, R. D. Rapid Ion Mobility Separations of Bile Acid Isomers Using Cyclodextrin Adducts and Structures for Lossless Ion Manipulations. *Anal Chem* **2018**, *90* (18), 11086–11091. https://doi.org/10.1021/acs.analchem.8b02990.

(32) Rose, B. S.; May, J. C.; Reardon, A. R.; McLean, J. A. Collision Cross-Section Calibration Strategy for Lipid Measurements in SLIM-Based High-Resolution Ion Mobility. *J Am Soc Mass Spectrom* **2022**, *33* (7), 1229–1237. https://doi.org/10.1021/jasms.2c00067.

(33) Kedia, K.; Harris, R.; Ekroos, K.; Moser, K. W.; DeBord, D.; Tiberi, P.; Goracci, L.; Zhang, N. R.; Wang, W.; Spellman, D. S.; Bateman, K. Investigating Performance of the SLIM-Based High Resolution Ion Mobility Platform for Separation of Isomeric Phosphatidylcholine Species. *J Am Soc Mass Spectrom* **2023**, *34* (10), 2176–2186. https://doi.org/10.1021/jasms.3c00157.

(34) Aderorho, R.; Lucas, S. W.; Chouinard, C. D. Separation and Characterization of Synthetic Cannabinoid Metabolite Isomers Using SLIM High-Resolution Ion Mobility-Tandem Mass Spectrometry (HRIM-MS/MS). *J Am Soc Mass Spectrom* **2024**. https://doi.org/10.1021/jasms.3c00419.

(35) Harrilal, C. P.; Gandhi, V. D.; Nagy, G.; Chen, X.; Buchanan, M. G.; Wojcik, R.; Conant, C. R.; Donor, M. T.; Ibrahim, Y. M.; Garimella, S. V. B.; Smith, R. D.; Larriba-Andaluz, C. Measurement and Theory of Gas-Phase Ion Mobility Shifts Resulting from Isotopomer Mass Distribution Changes. *Anal Chem* **2021**, *93* (45), 14966–14975. https://doi.org/10.1021/acs.analchem.1c01736.

(36) Valentine, S. J.; Clemmer, D. E. Treatise on the Measurement of Molecular Masses with Ion Mobility Spectrometry. *Anal Chem* **2009**, *81* (14), 5876–5880. https://doi.org/10.1021/ac900255a.

(37) Harrilal, C. P.; Garimella, S. V. B.; Chun, J.; Devanathan, N.; Zheng, X.; Ibrahim, Y. M.; Larriba-Andaluz, C.; Schenter, G.; Smith, R. D. The Role of Ion Rotation in Ion Mobility: Ultrahigh-Precision Prediction of Ion Mobility Dependence on Ion

Mass Distribution and Translational to Rotational Energy Transfer. *Journal of Physical Chemistry A* **2023**, *127* (25), 5458–5469. https://doi.org/10.1021/acs.jpca.3c01264.

(38) Wojcik, R.; Nagy, G.; Attah, I. K.; Webb, I. K.; Garimella, S. V. B.; Weitz, K. K.; Hollerbach, A.; Monroe, M. E.; Ligare, M. R.; Nielson, F. F.; Norheim, R. V.; Renslow, R. S.; Metz, T. O.; Ibrahim, Y. M.; Smith, R. D. SLIM Ultrahigh Resolution Ion Mobility Spectrometry Separations of Isotopologues and Isotopomers Reveal Mobility Shifts Due to Mass Distribution Changes. *Anal Chem* **2019**, *91* (18), 11952–11962. https://doi.org/10.1021/acs.analchem.9b02808.

(39) Viehland, L. A. Mobilities of Isotopic Ions in Gases. *International Journal for Ion Mobility Spectrometry* **2016**, *19* (1), 11–14. https://doi.org/10.1007/s12127-015-0186-8.

(40) Kirk, A. T.; Raddatz, C. R.; Zimmermann, S. Separation of Isotopologues in Ultra-High-Resolution Ion Mobility Spectrometry. *Anal Chem* **2017**, *89* (3), 1509–1515. https://doi.org/10.1021/acs.analchem.6b03300.

(41) Williamson, D. L.; Nagy, G. Isomer and Conformer-Specific Mass Distribution-Based Isotopic Shifts in High-Resolution Cyclic Ion Mobility Separations. *J Amer Soc Mass Spectrom.* **2024**, https://doi.org/10.1021/jasms.4c00082.

(42) Williamson, D. L.; Bergman, A. E.; Heider, E. C.; Nagy, G. Experimental Measurements of Relative Mobility Shifts Resulting from Isotopic Substitutions with High-Resolution Cyclic Ion Mobility Separations. *Anal Chem* **2022**, *94* (6), 2988–2995. https://doi.org/10.1021/acs.analchem.1c05240.

(43) Pathak, P.; Baird, M. A.; Shvartsburg, A. A. Structurally Informative Isotopic Shifts in Ion Mobility Spectra for Heavier Species. *J Am Soc Mass Spectrom* **2020**, *31* (1), 137–145. https://doi.org/10.1021/jasms.9b00018.

(44) Pathak, P.; Baird, M. A.; Shvartsburg, A. A. Identification of Isomers by Multidimensional Isotopic Shifts in High-Field Ion Mobility Spectra. *Anal Chem* **2018**, *90* (15), 9410–9417. https://doi.org/10.1021/acs.analchem.8b02057.

(45) Schaefer, C.; Kirk, A. T.; Allers, M.; Zimmermann, S. Ion Mobility Shift of Isotopologues in a High Kinetic Energy Ion Mobility Spectrometer (HiKE-IMS) at Elevated Effective Temperatures. *J Am Soc Mass Spectrom* **2020**, *31* (10), 2093–2101. https://doi.org/10.1021/jasms.0c00220.

(46) Pathak, P.; Shvartsburg, A. A. High-Definition Ion Mobility/Mass Spectrometry with Structural Isotopic Shifts for Nominally Isobaric Isotopologues. *Journal of Physical Chemistry A* **2023**, *127* (17), 3914–3923. https://doi.org/10.1021/acs.jpca.3c01792.

(47) Pathak, P.; Sarycheva, A.; Baird, M. A.; Shvartsburg, A. A. Delineation of Isomers by the 13C Shifts in Ion Mobility Spectra. *J Am Soc Mass Spectrom* **2021**, *32* (1), 340–345. https://doi.org/10.1021/jasms.0c00350.

(48) Williamson, D.; Windsor, H.; Nagy, G. Isolating the Contributions from Moments of Inertia in Isotopic Shifts Measured by High-Resolution Cyclic Ion Mobility Separations. *J Am Soc Mass Spectrom* **2024**.

(49) Bilbao, A.; Gibbons, B. C.; Stow, S. M.; Kyle, J. E.; Bloodsworth, K. J.; Payne, S. H.; Smith, R. D.; Ibrahim, Y. M.; Baker, E. S.; Fjeldsted, J. C. A Preprocessing Tool for Enhanced Ion Mobility-Mass Spectrometry-Based Omics Workflows. *J Proteome Res* **2022**, *21* (3), 798–807. https://doi.org/10.1021/acs.jproteome.1c00425.

Table of Contents Graphic